Research Square

Preprints are preliminary reports that have not undergone peer review.
They should not be considered conclusive, used to inform clinical practice,
or referenced by the media as validated information.

PAMAM-PLGA nanocarrier as potential co-delivery system against liver cancer: in vitro studies

Elahe Sadat Zahiroddini
Islamic Azad University, Karaj
Fereshteh Rahmati
Islamic Azad University, Karaj
Asghar Narmani
Tehran University of Medical Sciences
Javad Mohammadnejad
mohamadnejad@ut.ac.ir

University of Tehran

Research Article

Keywords: PLGA-PAMAM nanocarrier, Co-delivery system, Controlled drug release, Liver cancer, Apoptosis

Posted Date: September 17th, 2026

DOI: https://doi.org/10.21203/rs.3.rs-10751344/v1

License: This work is licensed under a Creative Commons Attribution 4.0 International License.
Read Full License

Additional Declarations: No competing interests reported.

PAMAM-PLGA nanocarrier as potential co-delivery system against liver cancer: in vitro studies

Elahe Sadat Zahiroddini [1], Fereshteh Rahmati [2,*], Asghar Narmani [3], Javad Mohammadnejad [4,*]

[1] Department of Genetics, NT.C., Islamic Azad University, Tehran, Iran

[2] Department of Biochemistry, NT.C., Islamic Azad University, Tehran, Iran

[3] Department of Medical Nanotechnology, School of Advanced Technologies in Medicine, Tehran University of Medical Sciences, 14177-55469, Tehran, Iran

[4] Department of Nanobiotechnology and Biomimetic, School of Life Science Engineering, College of interdisciplinary Science and Technology, University of Tehran, Tehran, Iran

Corresponding authors:

Javad Mohammadnejad: mohamadnejad@ut.ac.ir

Fereshteh Rahmati: fereshtehrahmati12345@iau.ac.ir

Abstract

Liver cancer has a high rate of incidence and mortality worldwide. The treatment of this cancer remains a big challenge in health sciences. Therefore, a nanocarrier based on polyamidoamine generation 4 (PAMAM G4) and polylactic-co-glycolic acid (PLGA) polymers was developed for co-delivery of sorafenib (Sor) and curcumin (Cur) to HepG2 liver cancer cells. The nanocarrier was characterized using FT-IR, DLS, TEM, and TGA analytical devices. The 231 nm hydrodynamic diameter, 100 nm to 250 nm diameter (TEM micrographs), globular and semi-globular shape, and 5.71% (Sor) and 4.39% (Cur) drug loading were observed for the fabricated nanocarrier. A 7.8% and 5.7% drug release was observed for Sor and Cur within 2 h, while it was pH-sensitive (51.6% for Sor and 58.9% for Cur at pH 5.0) in acidic conditions under the same time. The MTT assay demonstrated 21.1%, 9.4%, and 4.3% cell viabilities after 24 h of treatment with a 200 nM concentration of PAMAM-PLGA-Sor-Cur. The RT-PCR technique indicated 6.9-, 6.1-, and 5.9-fold enhancement in the expression of Caspase9, P53, and Bax apoptotic genes after treatment with the nanocarrier, respectively. Above 6-fold reduction observed in the expression of the Bcl2 anti-apoptotic gene. The fabricated co-drug-loaded nanocarrier would be a potential DDS for the suppression of liver cancer.

Keywords: PLGA-PAMAM nanocarrier; Co-delivery system; Controlled drug release; Liver cancer; Apoptosis

1. Introduction

Cancer remains a most challenging issue correlated with human health. This malignancy has a high rate of prevalence and mortality worldwide [1, 2]. Next to cardiovascular diseases, cancer is the second leading cause of death. The abnormal growth and proliferation of any of the various types of cells in the human body, which results in the formation of a tumor [2, 3]. Genetic disorders (such as inheritance and mutation), environmental factors (such as air pollution, chemicals, alcohol consumption, smoking, harmful irradiations), unusual diet habits, and sedentary lifestyle are mentioned as potential factors for cancer incidence and mortality [4, 5]. According to the statistics, more than 19.3 million cancer cases is occurred in 2024, which will increase to above 20 million in 2025. Moreover, approximately 2,041,910 new cancer cases and 618,120 cancer deaths are projected for the United States in 2025 based on the report of the American Cancer Society [6, 7]. Besides, above 35.5 million new cancer cases and 18.5 million are globally projected in 2050 [7,

8]. Among malignancies, liver cancer has raised concerns and is mentioned the fourth leading cause of death worldwide. This cancer accounts for approximately 800,000 new cases and more than 700,000 deaths across the world [9, 10]. Liver cancer is divided into four types: intrahepatic cholangiocarcinoma, hepatocellular carcinoma, hemangiosarcoma, and angiosarcoma [10].

On the other hand, there is a wide variety of modalities for cancer treatment, such as surgery, radiotherapy, and chemotherapy; however, the challenges associated with their deficiencies are considered major concerns for these modalities [11, 12]. To put it in a more vivid picture, surgery causes damage to healthy tissue during the operation, which leads to the formation of a lesion in the target organ [11, 13]. Radiotherapy can break the double-stranded DNA in normal cells, induce uncontrolled cell division, and make the cells carcinogenic. Other adverse effects of radiation therapy on patients include hair loss, anorexia, diarrhea, and vomiting [14]. Regarding chemotherapy, the use of chemotherapeutics results in remarkable adverse effects, like immunogenicity and loss of appetite. Moreover, the applied chemotherapeutics possess low solubility, weak stability, and fast body clearance, which reduces their functionality in the cancer treatment after intravenous (IV) administration [15, 16]. As a result, there is a fundamental requirement for the development of breakthrough technologies in cancer therapy. One of the most prominent approaches in cancer treatment is the use of nanotechnology and the development of nanoparticle-based procedures [17, 18].

Nanotechnology offers a promising field of science to develop high-tech and breakthrough tools for the diagnosis and treatment of diseases, especially cancer. Among nanoparticles, dendrimers are the most practical platforms for the fabrication of drug delivery systems (DDSs) [15]. Polyamidoamine generation 4 (PAMAM G4) dendrimers, as a type of chemopolymer, have a globular and hyperbranched shape, nanometric size (about 4.4 nm in diameter), serum stability, mechanical strength, hydrophilicity, reliable mocoadhesivity, and cellular uptake [15, 19, 20]. The surface amino functional groups of PAMAM nanoparticles provide an opportunity for surface engineering (modification and functionalization), which paves the way for conjugation of bioactive materials on their surface to improve the efficiency of DDS [21]. On the other side, polylactic-co-glycolic acid (PLGA), as a polymeric biomaterial, has lots of applications in pharmaceutical and biomedical sciences [22]. This biopolymer possesses appropriate physicochemical characteristics, such as surface functional groups (carboxylic acid), solubility, viscosity, crystallinity, glass transition temperature (Tg), and mechanical strength. PLGA has

potential biomedical features, like biocompatibility, biodegradability, and non-immunogenicity, which further improve its practicality for the development of efficient DDSs [23, 24].

The surface amino groups of PAMAM nanoparticles could cause toxicity in normal cells after administration. These positively charged groups could be covered by a biocompatible material to reduce the immunogenicity and cell cytotoxicity. PLGA would be a potential biopolymer for this purpose. The combination of PAMAM-PLGA increases the drug loading capacity, reduces the drug release rate, and maximizes enhanced permeability and retention (EPR) effect [25, 26]. This DDS may potentially apply for the efficient delivery of bioactive/therapeutics to the site of action in cancerous tissues. Sorafenib (Sor) and curcumin (Cur) are the therapeutics for cancer therapy. The anticancer function of Sor includes suppression of serine/threonine kinase (Raf-1 and B-Raf kinases), induction of apoptosis, suppression of tumor cell proliferation, and mitigating angiogenesis [27, 28]. On the other hand, Cur may suppress the STAT3, NF-κB, VEGF, transcription factors (like nuclear factor-κβ), and growth factors (like GF-β1 and TNF-α) signaling pathways to prevent cancer cell proliferation, development, and progression [29, 30]. Cur has antioxidant function and codelivery of this bioactive with Sor would potentially enhance the anticancer function of both therapeutics. PAMAM-PLGA nanocarrier could improve the physicochemical features of these therapeutics; for instance, Sor and Cur have low solubility and stability in the serum, and this drawback could be solved with PAMAM-PLGA DDS [31].

In the current study, a nanocarrier based on PAMAM-PLGA copolymers was developed for the combined delivery of Sor and Cur to liver cancer cells. After preparing the DDS, various analytical devices, including FT-IR, DLS, TEM, and TGA, were applied for the characterization of the fabricated nanocarrier. Drug loading capacity and drug release profile of the DDS were evaluated. Biomedical analyses (MTT assay and RT-PCR technique) were carried out to determine the cancer cell inhibition and apoptosis-inducing capability of the prepared nanocarrier on HepG2 liver cancer cells.

2. Materials and methods

2.1. Chemicals and apparatus

PAMAM G4 dendrimer dissolved in methanolic solution (Mw: 14,215 Da), PLGA powder (50:50, Mw: 30,000 to 60,000 Da), 1-Ethyl-3-(3-dimethyl-aminopropyl) carbodiimide (EDC), N-hydroxysuccinimide (NHS), Sor, Cur, and dimethyl sulfoxide (DMSO) were bought from Sigma-Aldrich. Besides, RPMI 1640 medium, fetal bovine serum (FBS), 3-(4,5-dimethylthiazol-2-yl)-

2,5-diphenyltetrazolium bromide (MTT), and dialysis membrane were purchased from Sigma Aldrich. The HepG2 human liver cancer cell lines and the MSC human normal cell lines were prepared from the Pasteur Institute, Iran.

Various analytical instruments were applied for the characterization of the prepared nanocarrier, including NanoDrop 2000c UV-Vis (Thermo Scientific), Fourier transform infrared (FT-IR) (Perkin-Elmer 843), dynamic light scattering (DLS) (NanoBrook 90 Plus, Brookhaven), transmission electron microscopy (TEM, Zeiss, Germany), and thermal gravimetric analysis (TGA) (STA 1500, Rheometric Scientific).

2.2. Synthesis of PAMAM-PLGA nanocarrier

The esterification reaction was carried out to fabricate the PAMAM-PLGA nanocarrier based on the following procedure. A 60 mg PLGA was dissolved in 10 mL DMSO under stirring at 90 rpm at room temperature to prepare a homogenous solution within 30 min. Next, a 5 mL solution of EDC/NHS (with a 2:1 molar ratio) was prepared in DI water and added to the PLGA-containing solution under stirring at 80 rpm, in dark circumstances, a nitrogen atmosphere, and room temperature for 3 h to activate the PLGA biopolymer. In the following, the solution of activated PLGA was transferred to the prepared PAMAM solution (10 μM concentration in 8 mL) dissolved in DMSO. The reaction of conjugation of PAMAM to PLGA was implemented at 80 rpm stirring, a dark condition, a nitrogen atmosphere, and room temperature for 48 h. In what follows, the unconjugated PLGA reactants were removed by centrifugation at 5,000 rpm for 4 min; at the wake of this process, half of the PAMAM-PLGA nanocarrier was collected and saved at 4 °C for analytical and biomedical analyses, and the other half was used for the rest of the nanocarrier preparation in the next steps.

2.3. Preparation of PAMAM-PLGA-Sor-Cur nanocarrier

In this phase of preparation, both Sor and Cur therapeutic agents were loaded in the fabricated PAMAM-PLGA nanocarrier. Briefly, 6 mg Sor was solubilized in 8 mL DMF/DMSO (1:1 ratio) under stirring at 80 rpm for 30 min to prepare a homogenous Sor-containing solution, which was followed by adding to a 10 mL mixture of PAMAM-PLGA under stirring at 90 rpm. This process was conducted at 37 °C for 24 h. Afterward, the unloaded Sor molecules were removed by applying a dialysis tube (cut-off 12,000 Da). This purification was performed at 1 L DI water (n=3) and 1 L PBS (n=3) under 50 rpm stirring at room temperature. Thereafter, half of the Sor-loaded PAMAM-

PLGA nanocarrier was removed and stored at 4 °C for implementing analytical and biomedical assessments, and the other half was applied for loading of Cur. For this process, 6 mg Cur was dissolved in 8 mL DI water and transferred to 10 mL of PAMAM-PLGA-Sor-containing solution, and the mixture was stirred at 90 rpm and 37 °C overnight. Next, the purification of Cur-loaded nanocarrier was done using a dialyzed tube submerged in 1 L DI water (n=3) and 1 L PBS (n=3) under 50 rpm stirring. Eventually, the prepared PAMAM-PLGA-Sor-Cur nanocarrier was stored at 4 °C for analytical and biomedical assessments.

2.4. Characterization of syntheses

2.4.1. FT-IR analysis

The FT-IR analysis was carried out to verify the formation/deformation of bonds, successful drug loading, and position of functional groups in the fabricated nanocarriers. This technique was performed based on the KBr pellet procedure in the wavelength range between 400 cm^{-1} and 4000 cm^{-1}.

2.4.2. DLS analysis

The DLS technique was performed to scrutinize two physicochemical properties of the prepared samples, including average hydrodynamic diameter and dispersity. The nM concentrations of the freshly prepared samples were firstly ultrasonicated at 37 °C for 20 min and then analyzed for the mentioned physicochemical properties at 37 °C in a quartz cuvette.

2.4.3. TEM analysis

The TEM analysis was conducted to evaluate the size, shape, and distribution of the prepared dual-drug-loaded nanocarrier. In practice, the prepared DDS was dispersed onto a copper grid and dried at 25 °C to remove the liquid of the nanocarrier, which followed by taking the micrograph of sample at an accelerating voltage of 120 kV.

2.4.4. TGA analysis

The TGA analysis was done to survey the drug loading capacity and thermal stability of the fabricated samples based on the following procedure. In practice, 1.5 to 3 mg of nanocarriers were placed on the pan of the device, and the heating process was employed at a temperature range from 50 °C to 600 °C at 10 °C/min rate and a constant nitrogen flow rate of 40 mL/min.

2.5. Drug release study

The drug release analysis was carried out to investigate the release profile of Sor and Cur from the fabricated PAMAM-PLGA-Sor-Cur nanocarrier in *in vitro* conditions using a shaker-incubator. This assessment was evaluated in PBS (simulation of the human body serum), at 120 rpm, a temperature of 37 °C (simulation of the human body temperature), pH of 7.4 (simulation of normal human body serum pH), pH of 6.0 (simulation of the cancerous microenvironment), and 5.0 (simulation of the intracellular endosomal pH). In brief, 5 mg of PAMAM-PLGA-Sor-Cur nanocarrier was suspended in 10 mL PBS and transferred into the dialysis tube (cut-off 12,000 Da) which was closed at one end. Next, the tube was submerged in 1000 mL PBS and put in a shaker-incubator (120 rpm, 37 °C, and pH 7.4). Thereafter, 10 µL of PBS was collected at different intervals of time (including 0.5, 1, 2, 3, 4, 8, 16, 32, and 64 h) and the same volume of PBS was replaced after each collection. Eventually, the release values were quantified after measuring the UV-vis absorption (Nano-drop UV-vis spectroscopy) of Sor and Cur in collected samples at 264 nm and 425 nm wavelengths. This release study was conducted at two acidic pHs.

2.6. Cell culture

The HepG2 human liver cancer cell lines and MSC human normal cell lines were bought from the Pasteur Institute, Iran. They were cultured in RPMI medium (Gibco, UK) supplemented with 10% FBS, 2mM glutamine, 100 $\mu g mL^{-1}$ streptomycin, and 100 IU mL^{-1} penicillin, and consequently, incubated at 37 °C and 5% CO_2 to grow.

2.7. Cell viability assay

The cell viability assessment was carried out to study the liver cancer cell inhibition ability of the fabricated nanocarriers, including the PAMAM, PAMAM-PLGA, PAMAM-PLGA-Sor, PAMAM-PLGA-Sor-Cur, Sor, and Cur, on HepG2 cells. The MSC normal cell lines were used as the control group. The cell viability analysis was performed by the MTT assay, which is a kind of colorimetric test [21]. MTT assay measures the activity of mitochondrial dehydrogenase through which the yellow color of MTT solution is modified to insoluble purple formazan crystals in live cells. In this assay, different concentrations of samples, including 50 nM, 100 nM, 150 nM, and 200 nM, were used for the incubation of cells at 24 h, 48 h, and 72 h post-treatment. Practically, 5,000 cells/100 µL of HepG2 and MSC cells were separately seeded to each well of 96-well microtiter plates, the cells were incubated at 37 °C and 5% CO_2 overnight for cell attachment. Next, different concentrations of samples were prepared in a serum-supplemented culture medium.

These samples were sterilized by a 0.2 mm filter, and their pH was adjusted to 7.4. Afterward, the culture medium of each well was replaced with 150 µL solution of the prepared samples, and the microtiter plates were incubated at 37 °C and 5% CO_2 for 24 h, 48 h, and 72 h. Then, after removing the medium of the wells at predetermined times, 200 µL of serum-free RPMI medium containing 0.5 mg MTT/mL was added to the wells, and the plates were incubated at 37 °C and 5% CO_2 for 4 h; at the end of this process, suspension liquid of wells was removed and 200 mL DMSO was added to the wells. The plates were incubated in light-protected circumstances for 20 min, followed by measuring the optical density (OD) of the plates at 570 nm using an ELISA reader. The cell viability values were calculated after comparison with control groups.

2.8. Gene expression assay

The qRT-PCR technique was employed to evaluate the relative expression levels of apoptotic (Caspase9, Bax, and P53) and anti-apoptotic (Bcl2) genes (Q Rotor-Gene, Qiagen, Iran) [32]. The IC_{50} concentrations of PAMAM-PLGA, PAMAM-PLGA-Sor, and PAMAM-PLGA-Sor-Cur samples were prepared for HepG2 cancer cells after 5 h of incubation based on the following procedure. Briefly, after incubation of cancer cells with the IC_{50} concentration of specimens, the RNX-PLUS solution was applied to submerge HepG2 cells and isolate the total RNA. Thereafter, 200 µL of chloroform was added to the mixture, and centrifugation was set at 13,000 rpm and 4 °C for 6 min. Next, the precipitate was mixed with isopropanol, the mixture was centrifuged at 13,000 rpm and 4 °C for 15 min, and 1 mL of ethanol 75% was added to the precipitate. Then, 1000 ng of total RNA was applied for the fabrication of the cDNA using reverse transcriptase: 10 µL of Master mix real-time, 7 µL double distilled, and 3 µL (10 ng) RNA were transferred into microtubes, and the qRT-PCR was carried out with a 14 µL of the reaction mixture, 1 µL of cDNA, 7 µL of low rox Master mix real-time, and 0.5 µL of forward primer (Caspase9: 5′TGGCTCCTGGTACGTTGA3′; P53: GGAGTATTTGGATGACAGAAAC; Bax: 5′TTTCTGACGGCAACTTCAACTG3′; Bcl2: 5′TCGCCCTGTGGATGACTGA3′; GAPDH: 5′GTGGTCTCCTCTGACTTCAAC3′) and 0.5 µL of reverse primer (Caspase9: 5′GAAACAGCATTAGCGACCCT3′; P53 gene: GATTACCACTGGAGTCTTC; Bax: 5′TCCAATGTCCAGCCCATGA3′; Bcl2: 5′CAGAGACAGCCAGGAGAAATCA3′; GAPDH: 5′GGAAATGAGGCTTGACAAAGTGG3′). At the wake of this process, the temperature was set for the RT-qPCR device: heating at 95 ºC for 10 min, 45 cycles at 95 ºC for 15 seconds, annealing at 59 ºC for 25 seconds, and elongation at 72 ºC for 30 seconds. Eventually, the relative gene

expression levels of apoptotic and anti-apoptotic genes were normalized to GAPDH, and the data were calculated as fold change compared with the control.

2.9. Statistical analysis

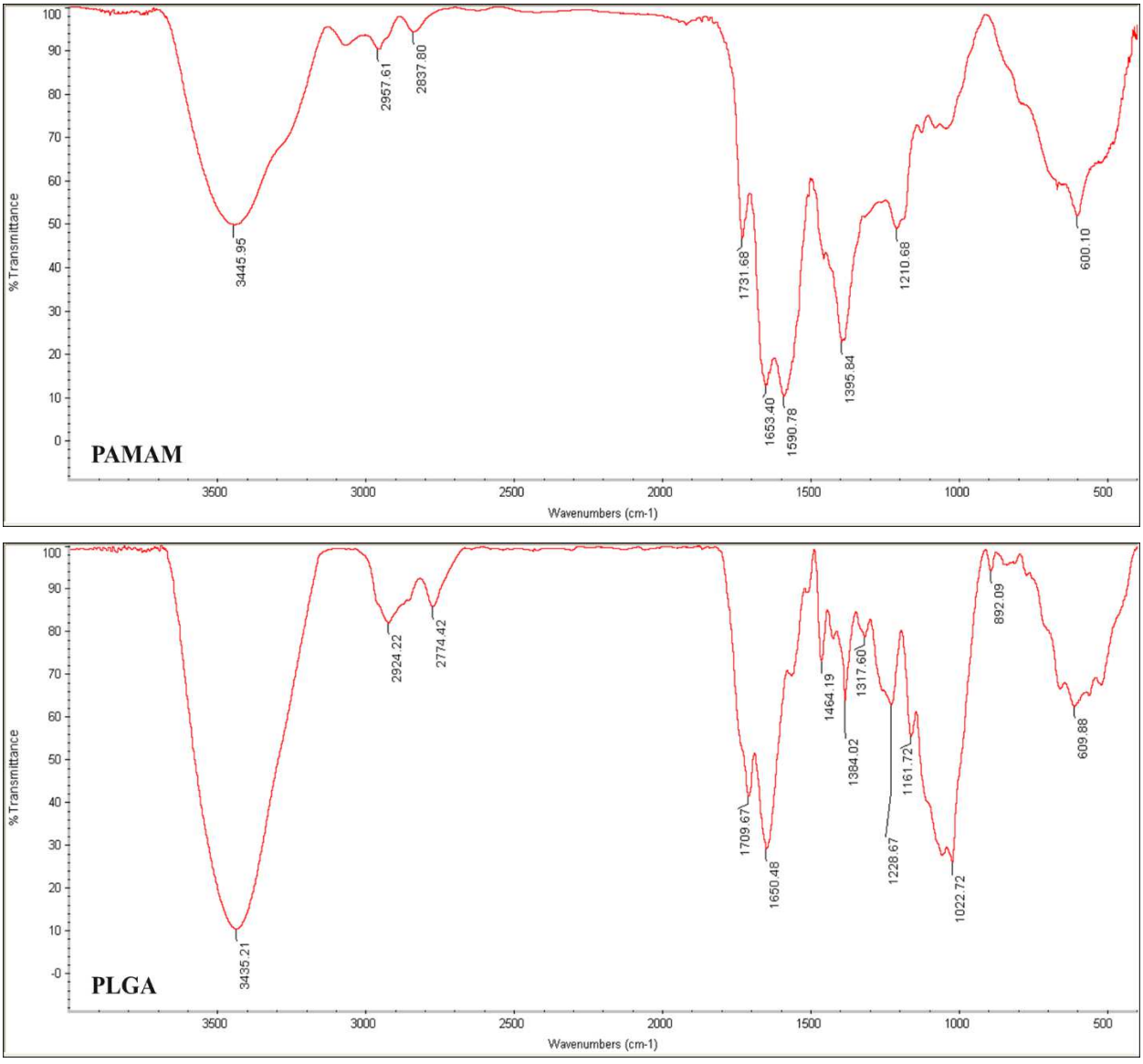
The analyses were triplicated, and the difference between groups was analyzed by the one-way ANOVA analysis with a considered significance at *$p < 0.05$.

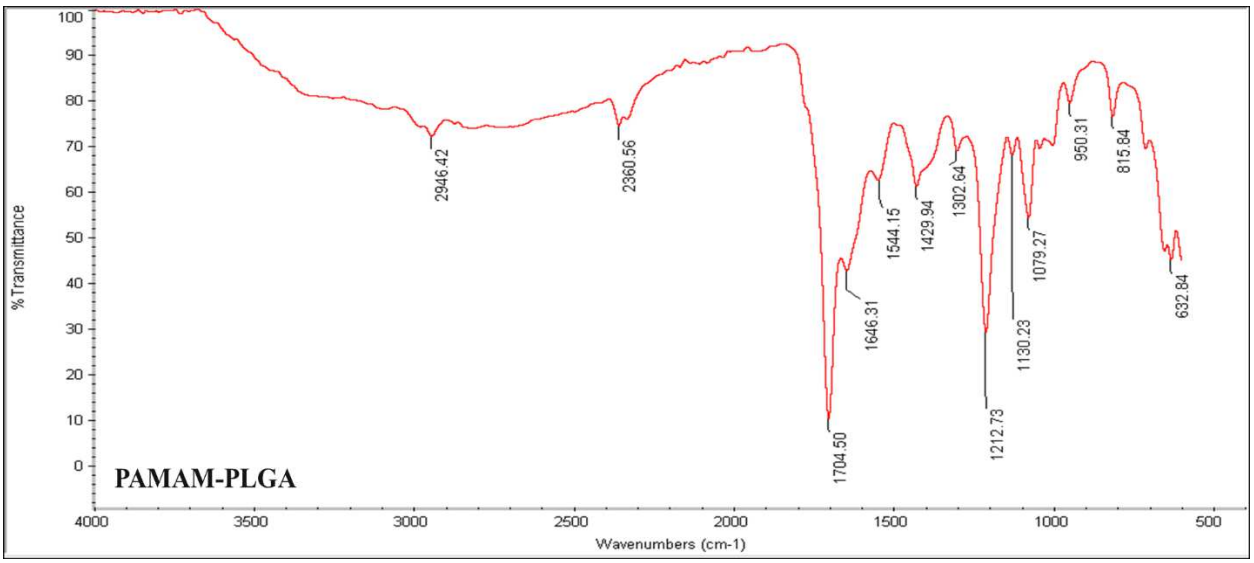
3. Results and discussion

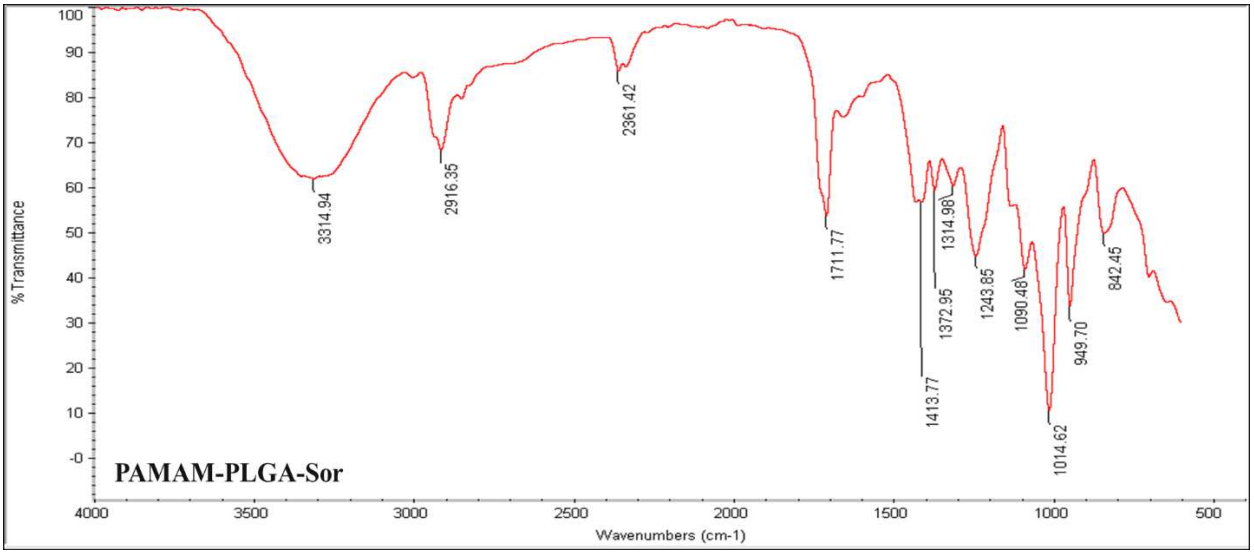
3.1. FT-IR analysis

FT-IR technique was carried out to confirm the formation/deformation of covalent/non-covalent bonds and successful drug loading to nanocarriers, including PAMAM, PLGA, PAMAM-PLGA, PAMAM-PLGA-Sor, and PAMAM-PLGA-Sor-Cur. The results of this analysis are indicated in Fig. 1. Based on the data, the spectrum of pure PAMAM demonstrated the characteristic peaks of C=O stretching vibrations at around 1653 cm^{-1} and N–H bending of N-substituted amide at around 1590 cm^{-1}, 1450 cm^{-1}, and 1395 cm^{-1} [32, 33]. Moreover, the absorption signals at around 3300 cm^{-1} and 3110 cm^{-1} were recorded owing to N–H stretch of amines and the anti-symmetric N–H stretch of substituted primary amine in PAMAM G4 [25]. Regarding the spectrum of pure PLGA, a sharp absorption signal at around 3150 cm^{-1} to 3650 cm^{-1} was assigned to the −OH group, whereas the intense characteristic peaks at around 1650 cm^{-1} and 1709 cm^{-1} were responsible for the C=O groups (stretching vibration) [22]. Additionally, the peaks at around 1022 cm^{-1} and 1226 cm^{-1} were registered owing to C−O stretching of ester groups and C−H groups in the pure PLGA, respectively [16, 22]. The spectrum of PLGA-PAMAM nanocarrier showed the absorption signals at around 3400 cm^{-1} to 3600 cm^{-1}, 1081 cm^{-1}, and 1194 cm^{-1} which were correlated with –OH groups, C−O stretching of ester groups, and C−H groups, respectively [23]. Besides, the signals at around 2630 cm^{-1} and 2930 cm^{-1} were due to stretching vibrations of the C−H groups and the combined signal of carbonyl groups in PLGA. The peak of −CH−NH−C=O amides bending was observed at around 1544 cm^{-1} in PAMAM-PLGA nanocarrier [23, 34]. Regarding the PAMAM-PLGA-Sor nanocarrier, a wide peak at around 3314 cm^{-1} was registered owing to OH stretching vibration of intermolecular hydrogen bonds between the drug and nanocarrier, while a peak at around 2947 cm^{-1} was associated with the C–H stretching band of aromatic and aliphatic C–H in Sor structure [35, 36]. On the other hand, PAMAM-PLGA-Sor-Cur nanocarrier did exhibit absorption peak at around 3312 cm^{-1} (vibration of phenolic O–H),

2847 cm^{-1} to 2918 cm^{-1} (aromatic C–H stretch vibrations), and 1707 cm^{-1} (C=O stretching), which were linked to Cur drug [37]. The peaks at around 1428 cm^{-1} to 1514 cm^{-1} were attributed to olefinic bending vibration of the C–H bond in the benzene ring, and the absorption signal at around 1373 cm^{-1} appeared owing to the C–C vibrations [37, 38].




% Transmittance
Wavenumbers (cm-1)
2946.42
2360.56
1704.50
1646.31
1544.15
1429.94
1302.64
1212.73
1130.23
1079.27
950.31
815.84
632.84
PAMAM-PLGA


% Transmittance
Wavenumbers (cm-1)
3314.94
2916.35
2361.42
1711.77
1413.77
1372.95
1314.98
1243.85
1090.48
1014.62
949.70
842.45
PAMAM-PLGA-Sor

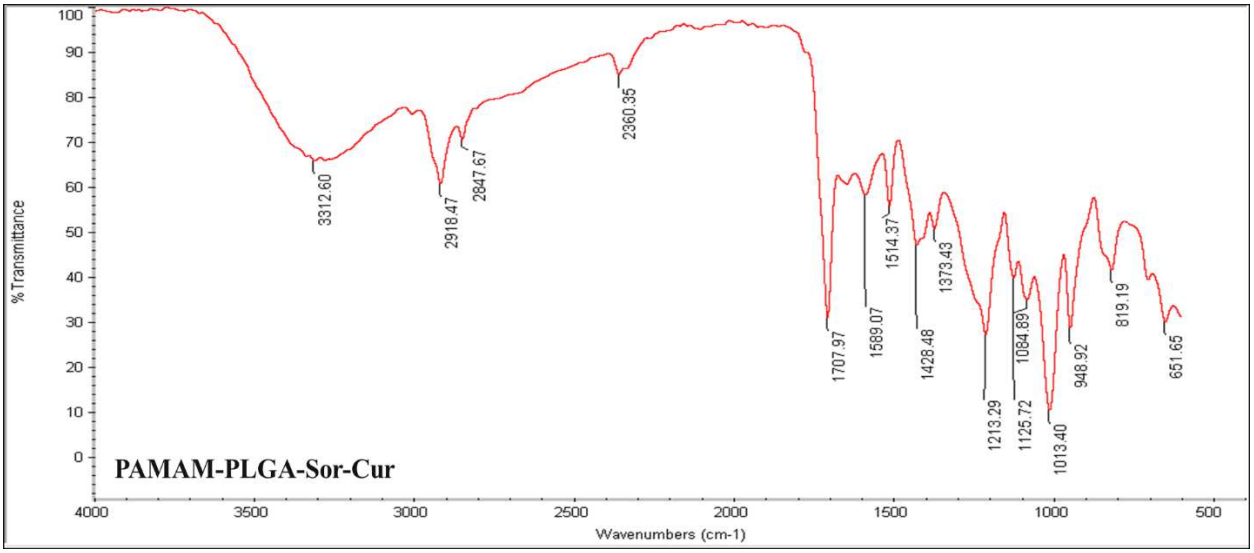

% Transmittance
Wavenumbers (cm-1)
3312.60
2918.47
2847.67
2360.35
1707.97
1589.07
1514.37
1428.48
1373.43
1213.29
1125.72
1084.89
1013.40
948.92
819.19
651.65
PAMAM-PLGA-Sor-Cur

Fig. 1. The FT-IR spectra of PAMAM, PLGA, PAMAM-PLGA, PAMAM-PLGA-Sor, and PAMAM-PLGA-Sor-Cur samples. The major characteristic peaks of the samples were registered on the graphs of spectra, which confirms the drug loading and formation/deformation of bonds.

3.2. DLS and TEM analyses

The average hydrodynamic diameter and polydispersity index (PDI) of the fabricated PAMAM-PLGA-Sor-Cur nanocarrier were scrutinized by the DLS technique. These features play a pivotal role in serum stability and solubility, drug loading capacity, penetration into the target cells, biosafety, drug release profile, biocompatibility, circulation time, and biodistribution of DDSs in the human body [39, 40]. The results of this analysis are presented in Fig. 2. According to the data, the average hydrodynamic diameter of the PAMAM-PLGA-Sor-Cur sample was determined to be 231 nm, which is appropriate for co-drug-loaded copolymeric DDS. The PDI of this nanocarrier was measured to be less than 0.2, which demonstrates its monodispersity. The nanometric size and monodispersity of DDSs have a momentous impact on the pharmacodynamics and pharmacokinetics of bioactive/therapeutics [41]. The nanocarriers with a nanometric diameter and appropriate PDI are favorable for efficient drug delivery to cancerous tissues and cells as they could evade the body clearance through ignoring the clearance system of the kidney, liver, and immune system cells (like macrophages) [41, 42]. On the other hand, the TEM technique was employed to determine the shape, size, and distribution of the fabricated nanocarriers. Based on this analysis, the size of PAMAM-PLGA-Sor-Cur was attained between 100 nm and 250 nm, which was in accordance with the result of DLS analysis. The shape of the nanocarrier was observed to be spherical and semispherical with reliable distribution. The nanometric DDSs with globular shape could efficiently penetrate into the cancerous tissue through the EPR effect since cancerous microvasculature has discontinuous walls with a cut-off range from 200 nm to 700 nm in diameter, which facilitate the penetration of DDSs with diameter below 700 nm [43-46].

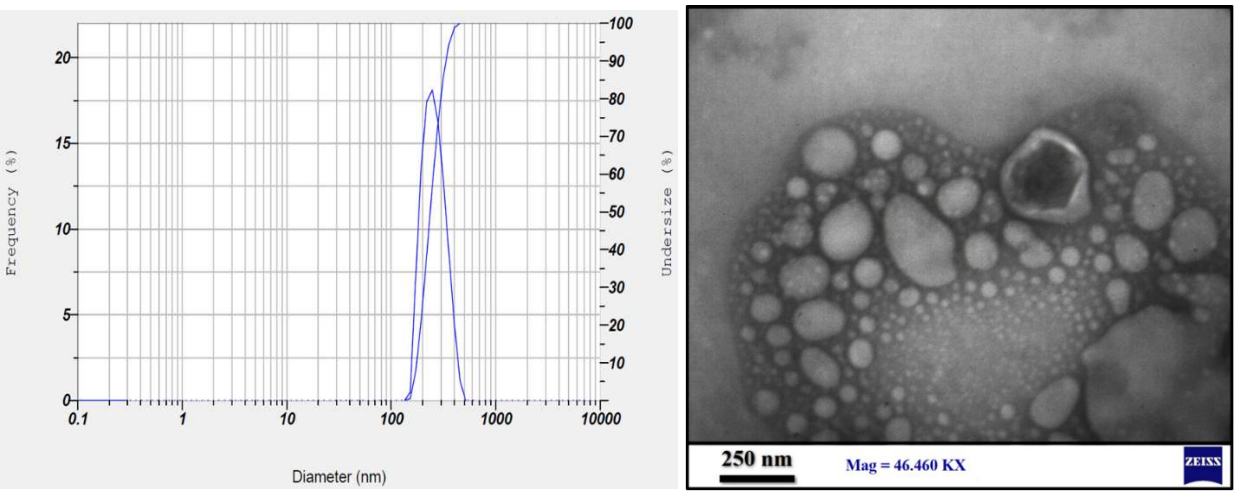


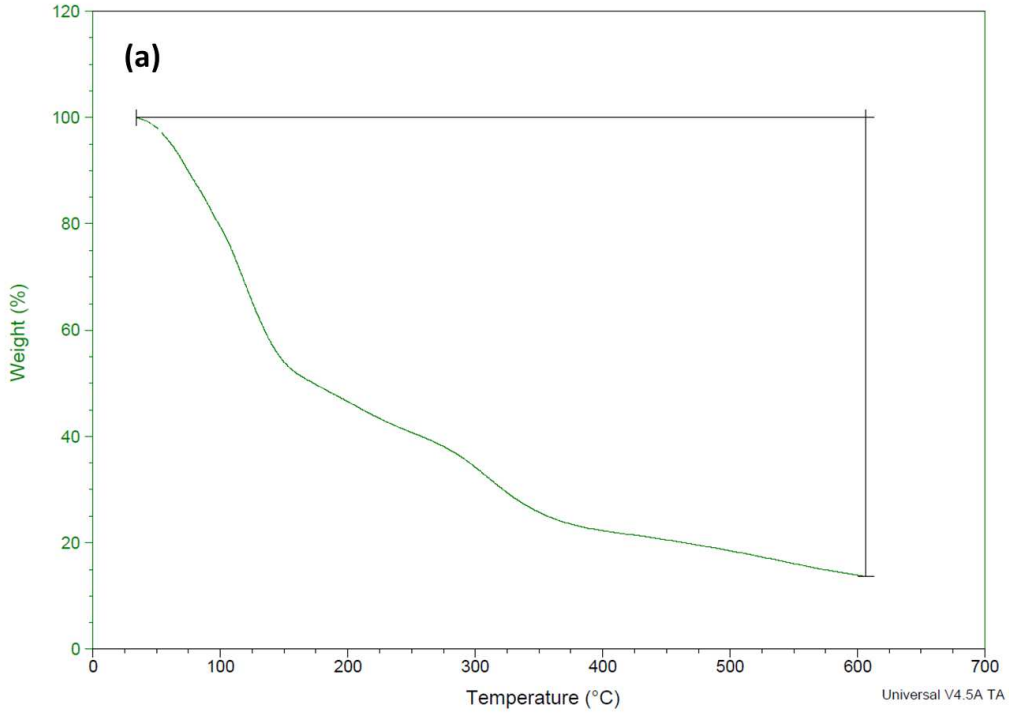
Fig. 2. The DLS and TEM results of the fabricated PAMAM-PLGA-Sor-Cur nanocarrier. The hydrodynamic diameter of the nanocarrier was measured at around 231 nm, and TEM micrographs indicated a size range from 100 nm to 250 nm with spherical and semi-spherical shapes.

3.3. TGA analysis and drug loading

The TGA analysis was carried out to investigate the thermal stability and drug content of the fabricated nanocarrier. The thermal stability and drug content of the nanocarrier are the most significant issues in the formulation process since they are the major determinants during the downstream processes and values of drug content in DDSs, respectively [12, 47]. Therefore, the thermal stability and drug loading capacity of PAMAM-PLGA (a), PAMAM-PLGA-Sor (b), and PAMAM-PLGA-Sor-Cur (c) samples were surveyed by a TGA device. This technique works based on the regular heating-cooling processes through which degradation rate and contents of Sor and Cur could be determined (Fig. 3). As can be seen in Fig. 3, there are two major weight losses for the PAMAM-PLGA sample, while the weight loss of PAMAM-PLGA-Sor and PAMAM-PLGA-Sor-Cur nanocarriers occurred in three steps. The PAMAM-PLGA sample had weight loss at around 90 to 150 ℃ and 200 to 350 ℃, in which about 50% and 25% weight losses were registered. The weight loss at around 90 ℃ (with about 3 to 5%) was owing to water evaporation, while others were correlated with the degradation of various elements of the samples. Regarding PAMAM-PLGA-Sor and PAMAM-PLGA-Sor-Cur specimens, the weight loss was observed at around 70 to 80 ℃ (5 to 10%), 100 to 250 ℃ (30 to 40%), and 250 to 500 ℃ (40 to 45%).

On the other hand, the total content of Sor and Cur therapeutics in PAMAM-PLGA-Sor and PAMAM-PLGA-Sor-Cur nanocarriers was determined based on the comparison of weight loss values between the samples, respectively. By comparing the weight loss values of PAMAM-PLGA

and PAMAM-PLGA-Sor nanocarriers, the difference was calculated at around 5.71% for Sor loading value in PAMAM-PLGA-Sor sample, and the difference of weight loss between PAMAM-PLGA-Sor and PAMAM-PLGA-Sor-Cur samples was quantified at 4.39% for Cur loading in PAMAM-PLGA-Sor-Cur nanocarrier. Sor and Cur, due to the weak solubility the human body serum, could agglomerate after intravenous administration. As a result, the circulation time of these therapeutics would be enhanced after loading in PAMAM-PLGA nanocarrier which in turn, guarantees the solubility and localization of drugs in the site of action as well as reduces the immunogenicity of these therapeutics [36, 48].



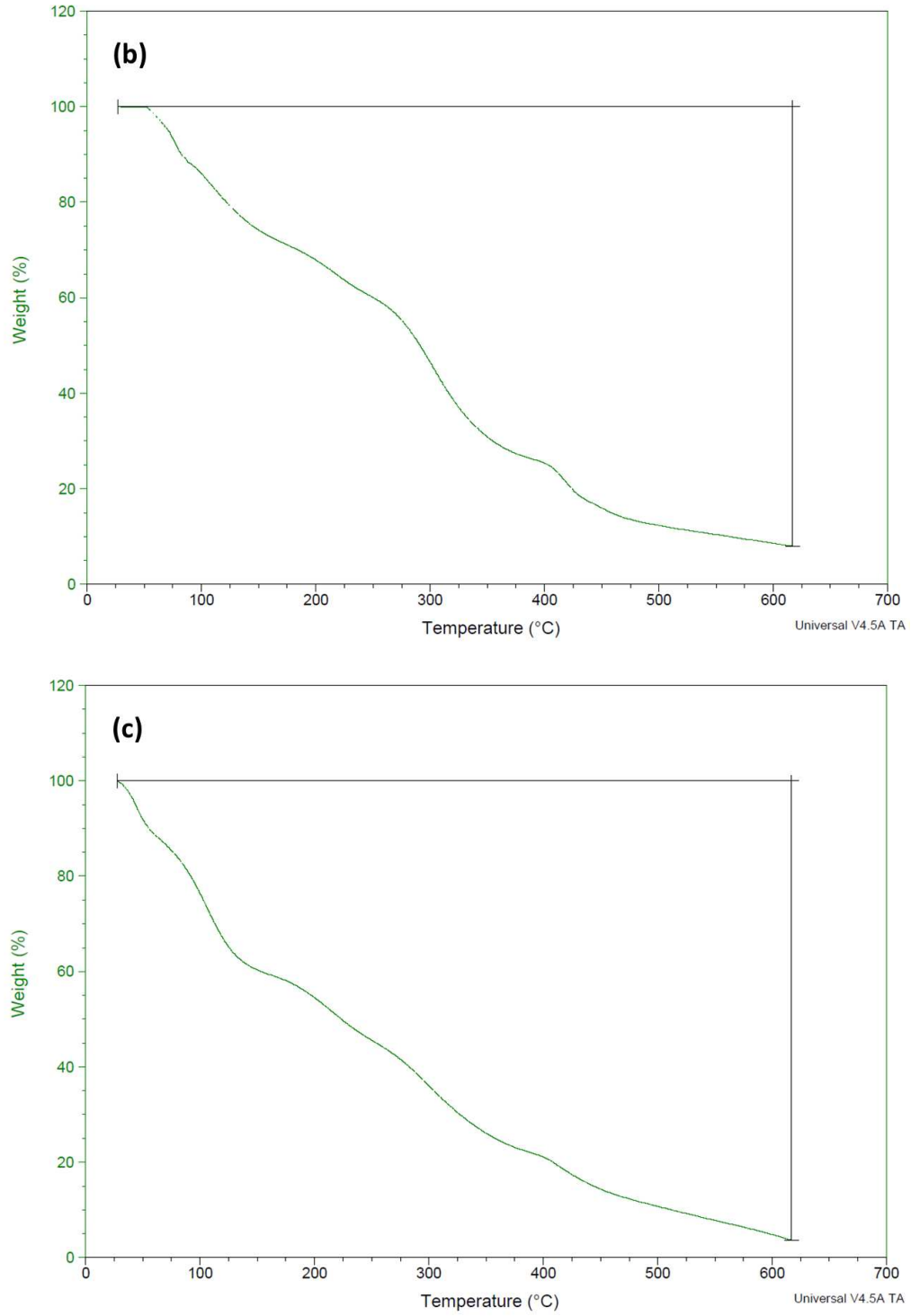


Fig. 3. The TGA data of PAMAM-PLGA, PAMAM-PLGA-Sor, and PAMAM-PLGA-Sor-Cur samples. The thermal stability and drug loading capacity of the fabricated nanocarriers were determined based on this technique. The Sor and Cur had 5.71% and 4.39% loading PAMAM-PLGA-Sor and PAMAM-PLGA-Sor-Cur samples, respectively.

3.4. Drug release study

The analysis is one of the most important tests in the fabricated DDSs since it is either directly or indirectly involved in drug dosage in the serum, immunogenicity, cytotoxicity, serum circulation time, and treatment efficiency at the site of action [49]. As a result, the drug release manner of Sor and Cur from PAMAM-PLGA-Sor and PAMAM-PLGA-Sor-Cur nanocarriers was investigated in PBS medium. The conditions of this assessment were 37 °C, 120 rpm, pH 7.4 (normal physiologic pH), and various acidic pHs (5.0 for simulation of endosomal microenvironment and 6.0 for simulation of tumorous microenvironment). The Sor release profile was evaluated in the PAMAM-PLGA-Sor sample, and the Cur release profile was assessed in the PAMAM-PLGA-Sor-Cur nanocarrier (Fig. 4). Based on the data, the burst Sor release was observed within the first 2 h for the PAMAM-PLGA-Sor nanocarrier, with more than 12% release at pH 7.4. The rate of release was reduced in the following period of time and reached nearly 39% after 8 h of incubation. Above 50% of the release occurred within 16 h of incubation, while it was observed after 2 h of incubation for pure Sor release; this output presents the impact of the nanocarrier in controlling the release of therapeutics. Regarding acidic pHs, 41% and 54% of Sor release were detected for PAMAM-PLGA-Sor nanocarrier after 4 h of incubation at pHs 6.0 and 5.0, respectively, whereas it was 21.5% for pH 7.4. These data support the pH-sensitive drug release manner of the nanocarrier. Regarding the PAMAM-PLGA-Sor-Cur nanocarrier, the potential controlled Cur release profile was attained within a 64 h of release period at pH 7.4. According to data, 17.5% release was measured for the Cur within the first 4 h at pH 7.4 while it was nearly 36% and 58.5% for pHs 6.0 and 5.0 at the same time, respectively. The release rate of pure Cur was about 7-fold faster than that of Cur release from PAMAM-PLGA-Sor-Cur nanocarrier after 2 h of incubation at pH 7.4, which further confirmed the controlled release manner of the nanocarrier compared with pure Cur release. On the other hand, the main reason behind the fast drug release manner of nanocarriers in acidic pH is the protonation of amino groups of PAMAM, which results in the steric modifications in the branches of PAMAM dendrimer and opening the cavity of PAMAM nanoparticles [50]. Since the cancerous cells have a high rate of anaerobic metabolism due to fast cell proliferation and formation of hypoxic conditions, a huge number of acidic metabolites is generated which, in turn, reduces the pH of the tumor microenvironment [50, 51].

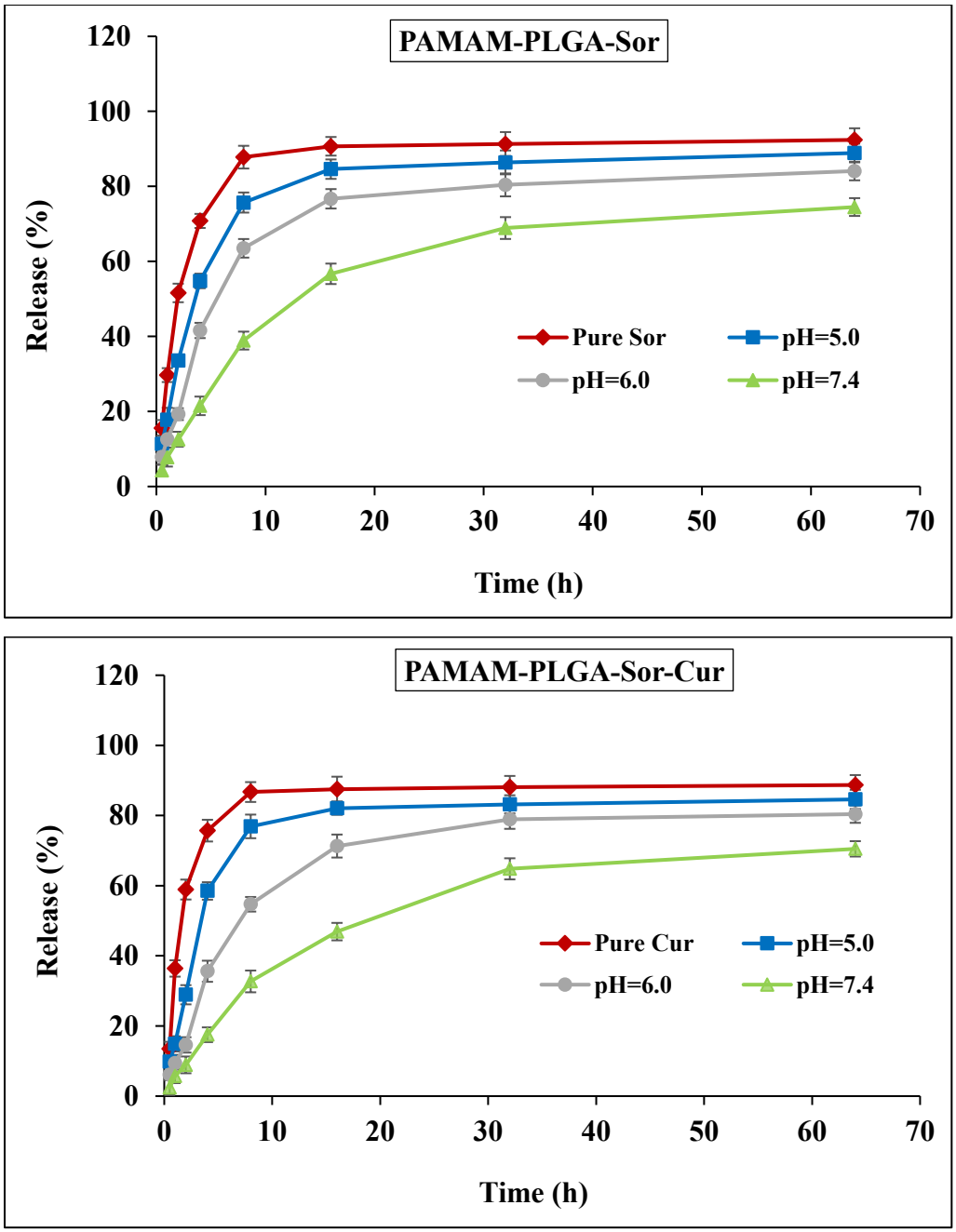


Fig. 4. The drug release profile of Sor and Cur therapeutics from PAMAM-PLGA-Sor and PAMAM-PLGA-Sor-Cur nanocarriers at normal and acidic pHs, 37 °C, and 120 rpm. Bot noncarriers demonstrated the controlled drug release profile at normal pH and fast drug release at acidic pHs.

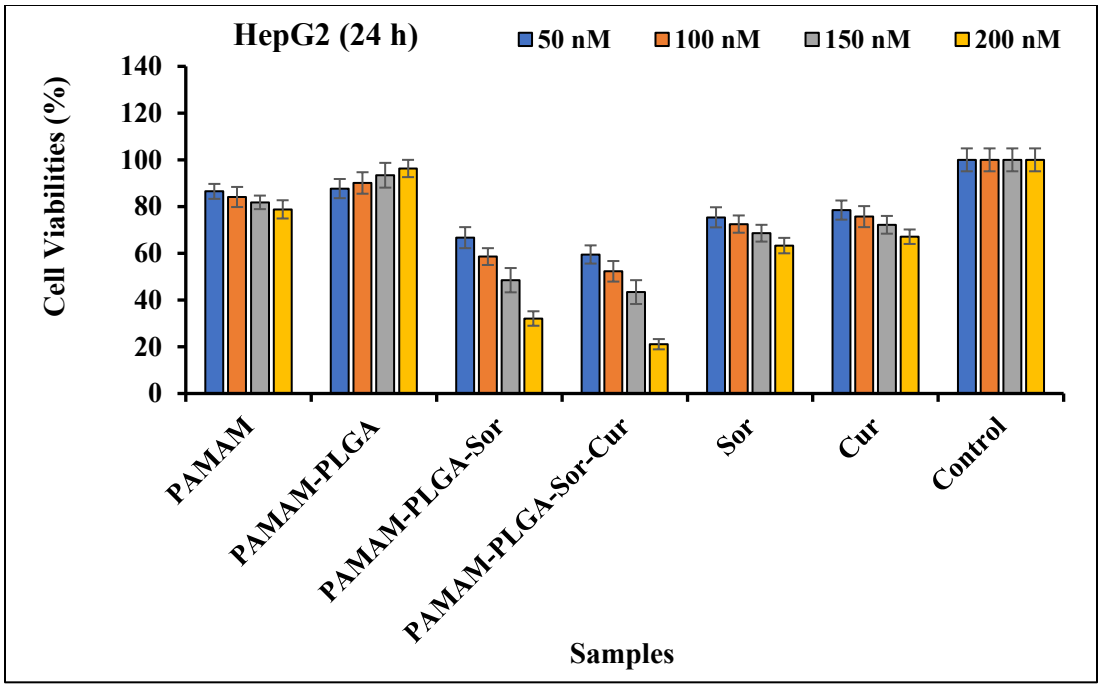
3.5. Cell viability assay

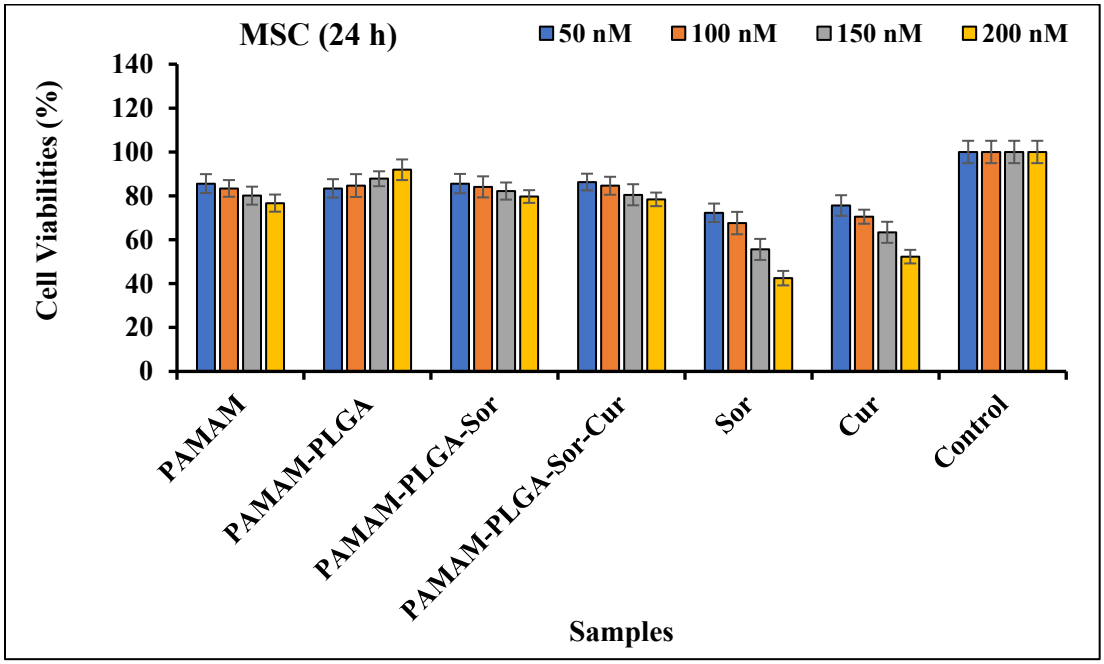
The MTT test was carried out to study the liver cancer cell-suppression performance of the fabricated nanocarriers, including the PAMAM, PAMAM-PLGA, PAMAM-PLGA-Sor, PAMAM-

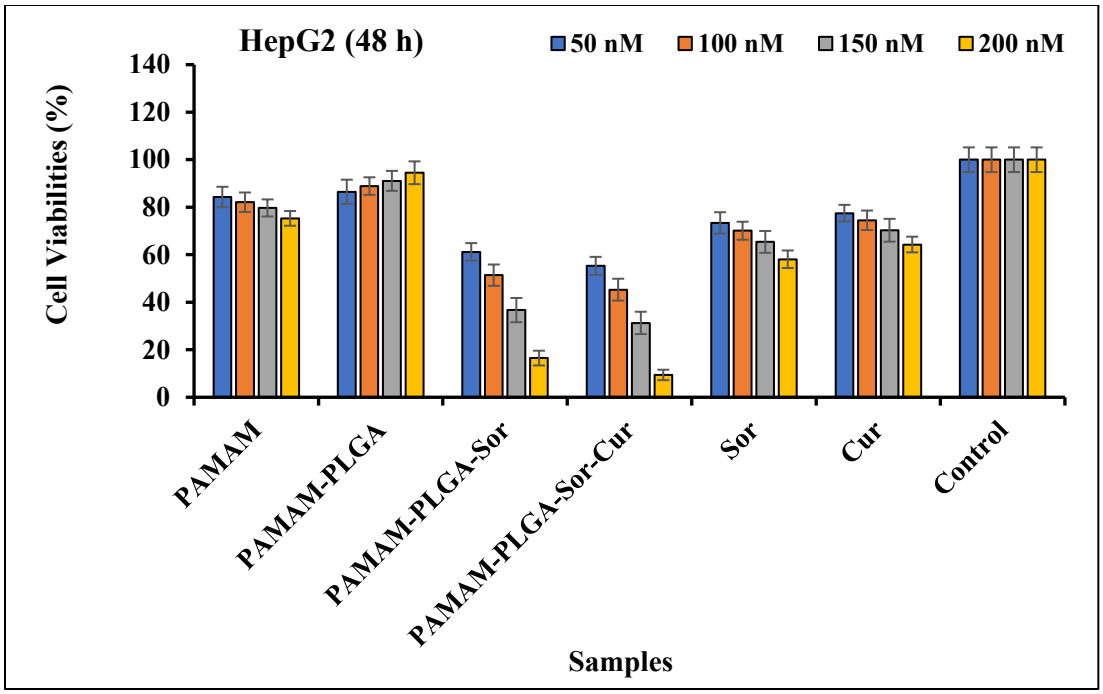
PLGA-Sor-Cur, Sor, and Cur, on HepG2 cell lines. The MSC normal cell lines were used as the control group. To implement this analysis, various concentrations of the fabricated specimens (50 nM, 100 nM, 150 nM, and 200 nM) were applied for 24 h, 48 h, and 72 h of incubation. Fig. 5 indicates the outputs of this test. From Fig. 5, it is crystal clear that there was a linear correlation between the concentrations of the specimens and toxicities; by increasing the concentration, the cell viability values were decreased for all samples, except for the PAMAM-PLGA nanocarrier. Among the samples, pure PAMAM had lower toxicity compared with others; this poor toxicity was probably owing to the presence of surface amino groups in PAMAM nanoparticles, which can interact with negatively charged proteoglycans on the surface of target cells. For example, the cell viability values of 86.5% to 78.8% were observed for HepG2 cells treated with PAMAM after 24 h of incubation with 50 nM and 200 nM concentrations, respectively. After modifying the surface of PAMAM with PLGA, the cell viability of HepG2 cells was increased from 87.7% (50 nM) to 96.3% (200 nM) after 24 h of treatment with PAMAM-PLGA. The enhancement was due to the biocompatibility of PLGA biopolymer, which could sterically cover the positively charged functional groups of PAMAM [5, 52, 53]. The remarkable reduction in cell viability values was observed for the PAMAM-PLGA-Sor sample, in which 32.1% cell viability was observed for HepG2 cells at 24 h post-treatment with 200 nM concentrations. The most considerable decline in cell viability values was measured for co-loaded PAMAM-PLGA-Sor-Cur nanocarrier which was ranged between 59.5% and 21.1% for minimum and maximum concentrations after 24 h of incubation in cancer cells, respectively. by comparing the impact of maximum concentration of PAMAM-PLGA-Sor and PAMAM-PLGA-Sor-Cur nanocarriers, it was observed that co-loaded nanocarrier reduced the cell viability of cancer cells by 11% compared with single drug-loaded nanocarrier, which states the considerable impact of dual loaded nanocarrier in induction of cytotoxicity in cancer cells [54]. The cell viability of HepG2 cells was further decreased after 48 h and 72 h of incubation with a 200 nM concentration of PAMAM-PLGA-Sor-Cur nanocarrier, with 9.4% and 4.3% cell viability, respectively. The synergistic impact of Sor and Cur was verified in this DDS, through which high toxicity could be observed for HepG2 cells [55]. The cell viability values did not demonstrate extensive change after incubation of cancer cells with pure Sor and Cur; as 63.3% and 67.1% cell viabilities were observed for cancer cells treated with 200 nM concentrations of pure Sor and Cur at 24 h post-treatment. By comparing the cell viability values of pure drugs with PAMAM-PLGA-Sor-Cur nanocarrier, it was crystal clear that drug-loaded

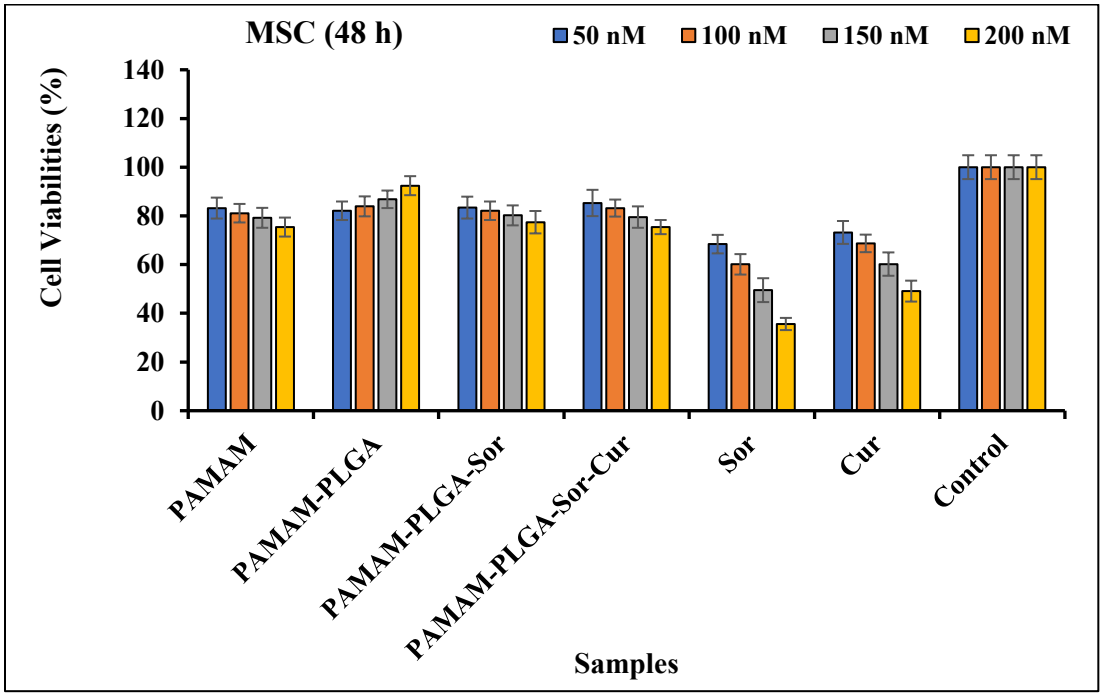
nanocarrier has better cytotoxicity function than pure drugs, which indicates how nanocarrier is practical for cancer suppression compared with applied pure drugs in chemotherapy [56]. On the other hand, PAMAM-PLGA-Sor and PAMAM-PLGA-Sor-Cur nanocarriers had considerably lower toxicity on MSC cells at maximum concentration than pure drug; to put it in a more vivid picture, the cell viability values of MSC cells were measured at around 79.7% and 78.4% after 24 h of incubation with 200 nM concentrations of PAMAM-PLGA-Sor and PAMAM-PLGA-Sor-Cur nanocarriers whereas it was 42.5% and 52.3% for pure Sor and Cur under the same conditions. These data verify the biocompatibility of the nanocarrier on normal cells and suggest that this nanoparticle-based DDS would be replaced with conventional chemotherapy in the clinic.

The IC_{50} values of PAMAM-PLGA-Sor and PAMAM-PLGA-Sor-Cur nanocarriers were calculated at around 141 nM and 122 nM for HepG2 cells after 24 h of treatment. The results of this analysis were in accordance with the findings of a study by Hosseini et al., in which they developed a folic acid (FA)-functionalized chitosan (CS)-poly lactic-co-glycolic acid (PLGA) nanocarrier for targeted delivery of sodium butyrate (NB) therapeutics to HepG2 cells. They indicated that CS-NB-PLGA-FA could result in 13% cell viability after 24 h of treatment with 400 nM concentrations [16]. Compared with our work, they used approximately 2-fold higher concentrations to reach IC_{50} concentrations, which could be owing to the co-loaded DDS in our study and the synergistic impact of Sor and Cur. Moreover, the outputs of our research were in line with the findings of a study by Sorasitthiyanukarn et al., in which they fabricated a CS/alginate DDS for the efficient delivery of curcumin diglutaric acid (Cur) against the liver (HepG2), breast (MDA-MB-231), and colorectal cancer (Caco-2) cells [57]. The Cur-loaded CS/alginate nanocarrier demonstrated potential biocompatibility and biodegradability in normal cells and cytotoxicity in cancer cells. The cell viability test indicated that Cur-loaded CS/alginate DDS had remarkable toxicity in three cancer cells at various Cur concentrations (from5 μg/mL to 10 μg/mL); it was about 60%, 70%, 68% cell viability for MDA-MB-231, HepG2, and Caco-2 cells at the high concentration, respectively, which was lower toxicity than our fabricated nanocarrier.


HepG2 (24 h)
50 nM
100 nM
150 nM
200 nM
Cell Viabilities (%)
140
120
100
80
60
40
20
0
PAMAM
PAMAM-PLGA
PAMAM-PLGA-Sor
PAMAM-PLGA-Sor-Cur
Sor
Cur
Control
Samples


MSC (24 h)
50 nM
100 nM
150 nM
200 nM
Cell Viabilities (%)
140
120
100
80
60
40
20
0
PAMAM
PAMAM-PLGA
PAMAM-PLGA-Sor
PAMAM-PLGA-Sor-Cur
Sor
Cur
Control
Samples


HepG2 (48 h)
50 nM
100 nM
150 nM
200 nM
Cell Viabilities (%)
140
120
100
80
60
40
20
0
PAMAM
PAMAM-PLGA
PAMAM-PLGA-Sor
PAMAM-PLGA-Sor-Cur
Sor
Cur
Control
Samples


MSC (48 h)
50 nM
100 nM
150 nM
200 nM
Cell Viabilities (%)
140
120
100
80
60
40
20
0
PAMAM
PAMAM-PLGA
PAMAM-PLGA-Sor
PAMAM-PLGA-Sor-Cur
Sor
Cur
Control
Samples

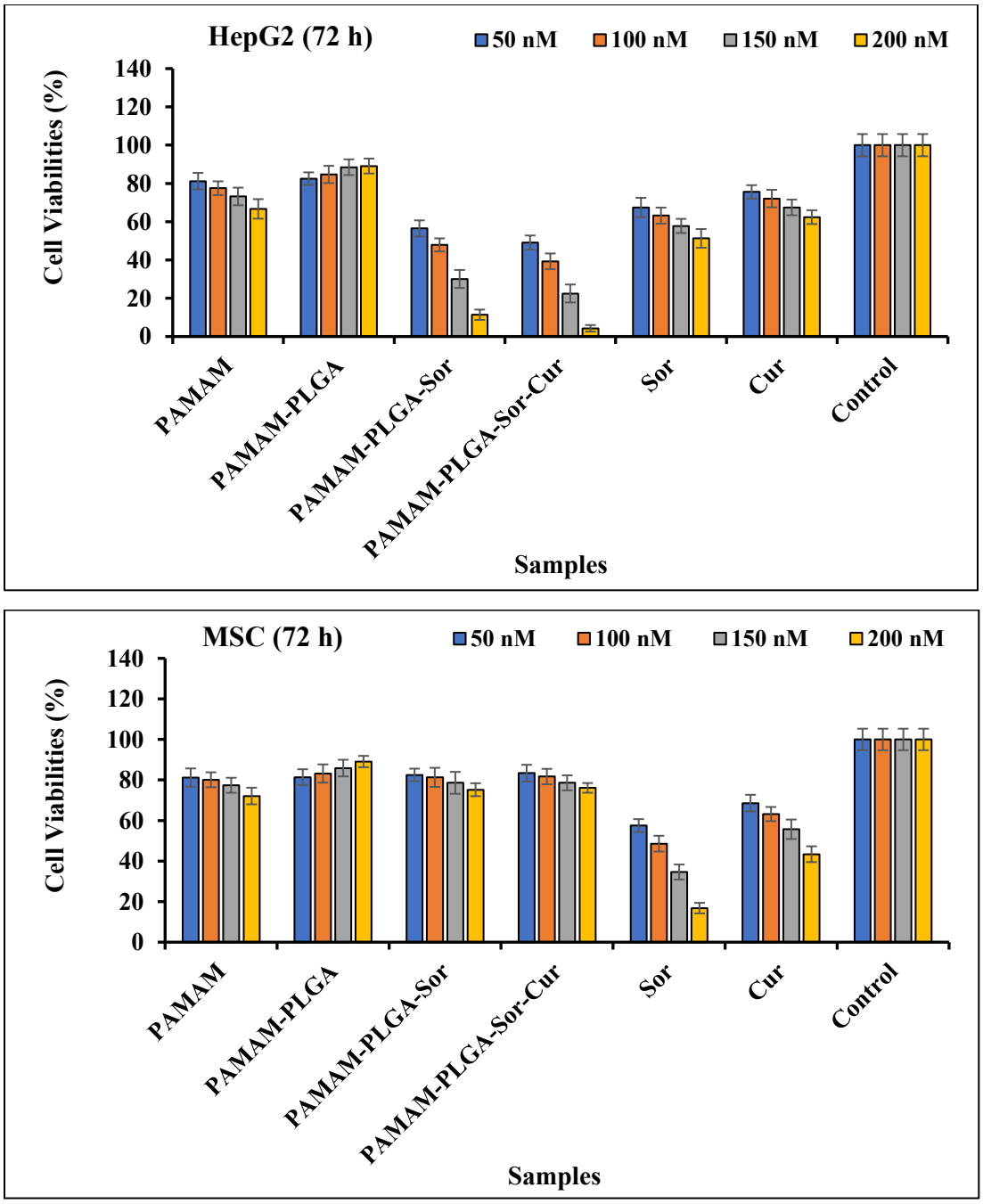
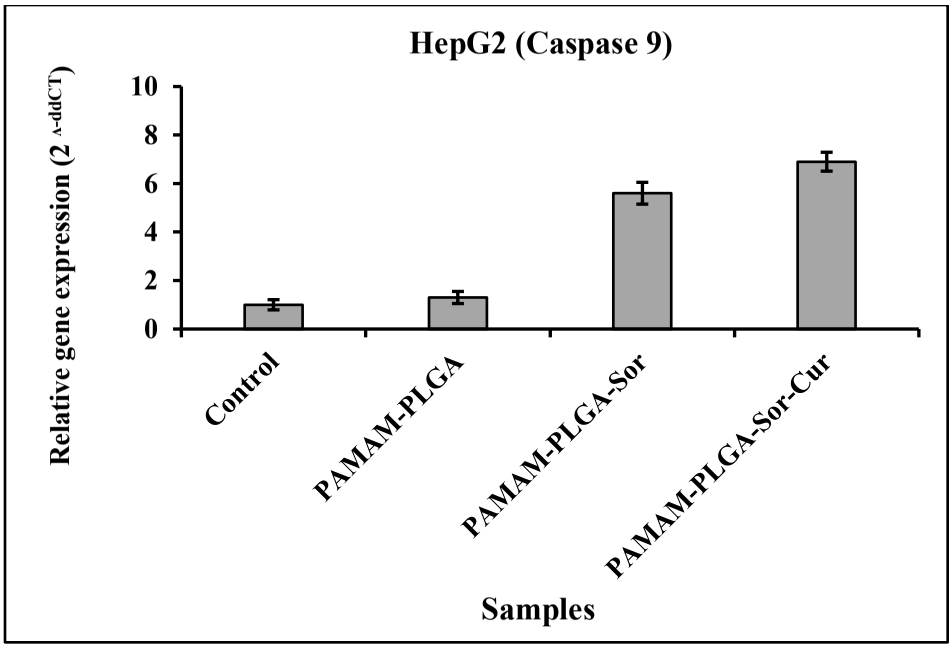
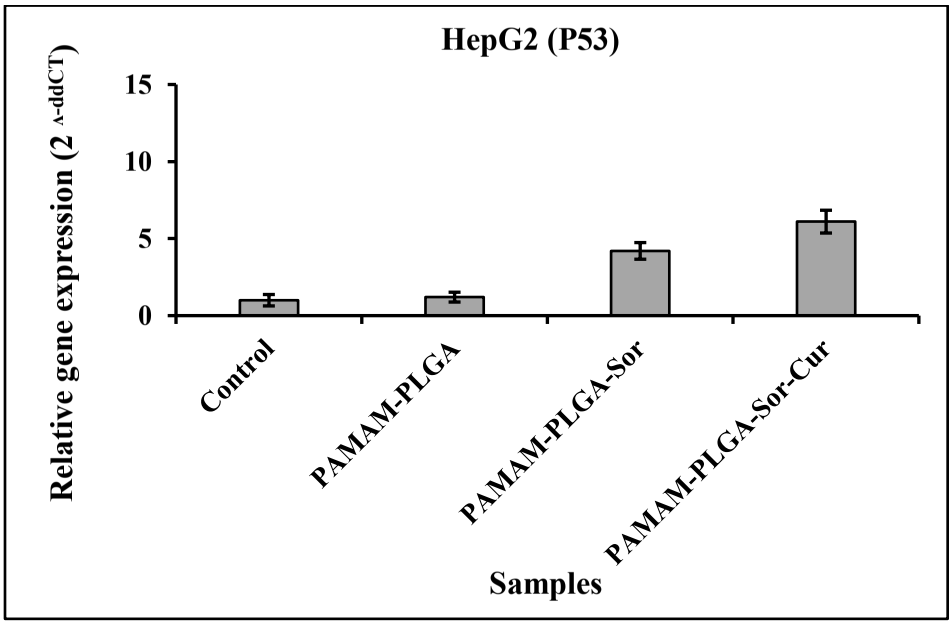


Fig. 5. The outputs of the MTT assay in HepG2 liver cancer cells and MSC normal cells. The 50 nM, 100 nM, 150 nM, and 200 nM concentrations of the prepared samples, including PAMAM, PAMAM-PLGA, PAMAM-PLGA-Sor, PAMAM-PLGA-Sor-Cur, Sor, and Cur, were used for the analysis after 24 h, 48 h, and 72 h of incubation.

3.6. Gene expression analysis

The qRT-PCR analysis was employed to survey the relative expression levels of apoptotic (Caspase9, P53, and Bax) and anti-apoptotic (Bcl2) genes in HepG2 cells after 5 h of incubation with the IC_{50} concentrations of samples, including PAMAM-PLGA, PAMAM-PLGA-Sor, and PAMAM-PLGA-Sor-Cur. Fig. 6 exhibits the results of this test. As can be seen in Fig. 6, the PAMAM-PLGA nanocarrier did not have an extensive effect on the expression values of apoptotic and antiapoptotic genes when compared with PAMAM-PLGA-Sor and PAMAM-PLGA-Sor-Cur nanocarriers. Based on results, PAMAM-PLGA led to 1.3-fold, 1.2-fold, and 1.4-fold enhancement compared with the control group in the expression levels of Caspase9, P53, and Bax genes, respectively. This result presents the biocompatibility of PAMAM-PLGA, which is primarily due to the presence of the PLGA biopolymer. After treatment of cancer cells with PAMAM-PLGA-Sor sample, the expression of Caspase9, P53, and Bax genes was considerably enhanced by 5.6-, 4.2-, and 4.6-fold, respectively, which further increased to 6.9-, 6.1-, and 5.9-fold after incubation with PAMAM-PLGA-Sor-Cur nanocarrier. These data show that the dual drug-loaded nanocarrier had a relatively 1.5-fold higher apoptosis inducing activity than that of the single drug-loaded nanocarrier, which exhibits the capability of the nanocarrier in the induction of apoptosis in HepG2 cells. Regarding the Bcl2 antiapoptotic gene, the expression was declined by 3-fold and 6-fold after treatment with PAMAM-PLGA-Sor and PAMAM-PLGA-Sor-Cur samples, respectively, which further confirms the apoptosis-inducing capability of the fabricated nanocarriers. The outputs of this study were consistent with the findings of a work by Shahpouri et al. in which the developed polyethylene glycol (PEG)-modified PAMAM G5 dendrimers crosslinked with a hypoxic azo linker for breast cancer therapy [58]. They delivered doxorubicin (Dox) to MDA-MB-231 breast cancer cells using μg/mL concentrations. Based on their data, the expression level of Bax was maximized by 12-fold after 24 h of treatment with a 10 μg/mL concentration. A slight enhancement was observed in the expression levels of the Caspase-3 gene as well [58]. Moreover, Sadeghi et al. have fabricated a PLGA-poly-ε-caprolactone (PCL) copolymeric DDS against lung cancer cells, by which Cur was delivered to A549 cells [59]. They applied the IC_{50} (100 nM) concentration of the PLGA-Cur-PCL to the induction of Caspase9 apoptotic and to the reduction of Bcl2 antiapoptotic genes. Above 6-fold enhancement in the expression of Caspase9 gene and more than 2-fold reduction in the expression of Bcl2 gene were observed after 5 h of incubation with the nanocarrier [59].


HepG2 (Caspase 9)
Relative gene expression (2 -ddCT)
10
8
6
4
2
0
Control
PAMAM-PLGA
PAMAM-PLGA-Sor
PAMAM-PLGA-Sor-Cur
Samples


HepG2 (P53)
Relative gene expression (2 -ddCT)
15
10
5
0
Control
PAMAM-PLGA
PAMAM-PLGA-Sor
PAMAM-PLGA-Sor-Cur
Samples

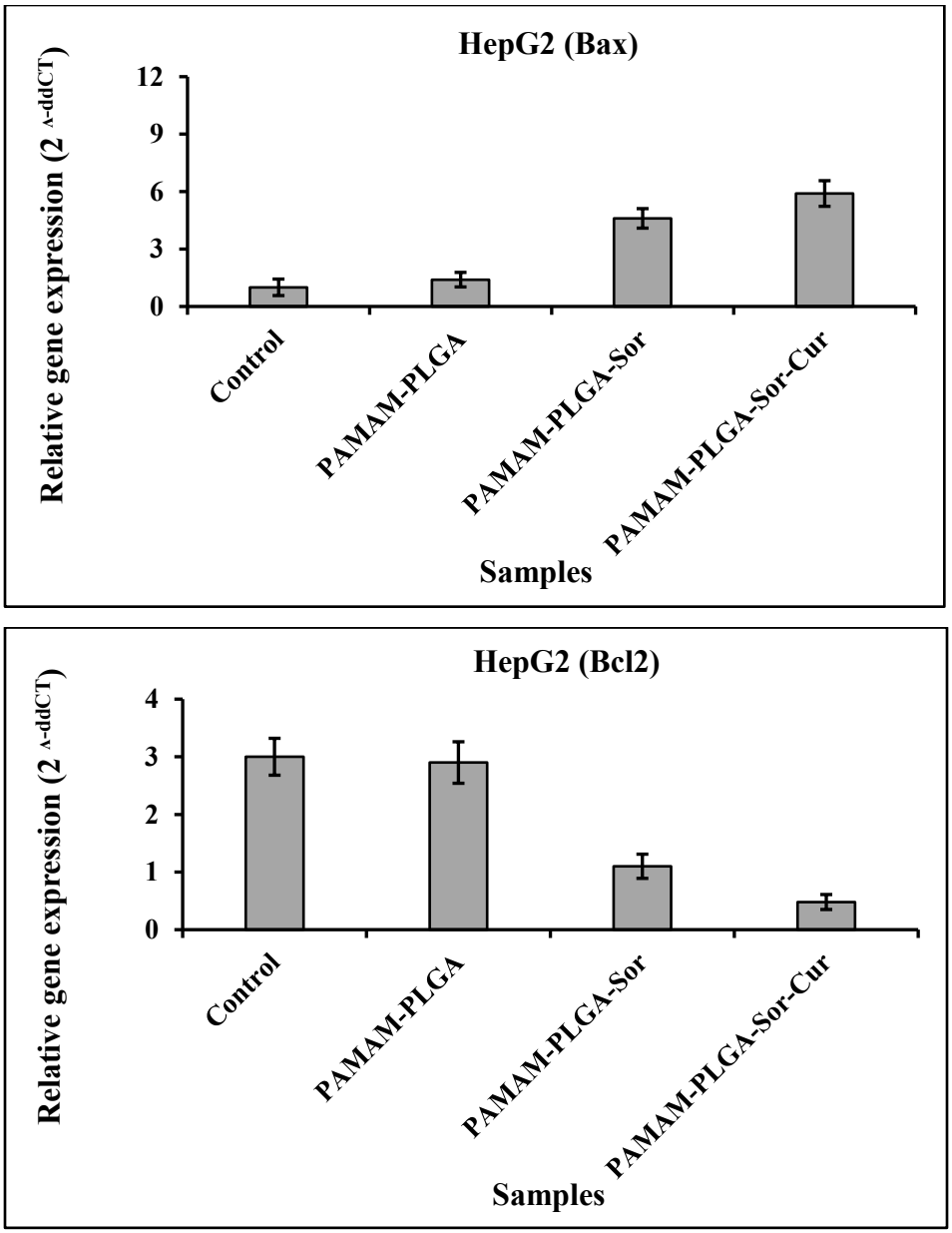


Fig. 6. The relative expression levels of apoptotic (Caspase9, Bax, and P53) and antiapoptotic (Bcl2) genes. This technique was done after 5 h of incubation with IC_{50} concentrations of nanocarriers (PAMAM-PLGA, PAMAM-PLGA-Sor, and PAMAM-PLGA-Sor-Cur). PAMAM-PLGA-Sor-Cur nanocarrier had better apoptosis-inducing performance than the single drug-loaded nanocarrier.

4. Conclusion

In this study, a novel DDS based on the PAMAM-PLGA polymeric nanosystem was fabricated for efficient co-delivery of Sor and Cur to HepG2 liver cancer cells. The prepared PAMAM-

PLGA-Sor-Cur nanocarrier was characterized with FT-IR, DLS, TEM, and TGA analytical devices. The successful nanocarrier fabrication, nanometric size, narrow distribution, and high drug loading capacity were measured for the nanocarrier. The controlled and pH-sensitive drug release profiles were observed for the nanocarrier, which is appropriate for safe drug carrying for acidic tissues of cancers. The MTT assay confirmed the efficient performance of the fabricated nanocarrier in the inhibition of cancer growth. The co-drug loaded nanocarrier had better cancer cell suppression capability than the single drug-loaded nanocarrier. RT-PCR technique demonstrated that PAMAM-PLGA-Sor-Cur DDS could exponentially induce the expression of Caspase9, P53, and Bax apoptotic gene and reduce the Bcl2 antiapoptotic gene in HepG2 cells. The fabricated PAMAM-PLGA-Sor-Cur nanocarrier has potential capacity in the suppression of liver cancer and would be replaced with the conventional chemotherapy approach in the future.

This project received no financial support

Ethics, Consent to Participate, and Consent to Publish declarations: not applicable

Data availability

The datasets used and/or analysed during the current study are available from the corresponding author on reasonable request.

References

1. Narmani, A. and S.M. Jafari, *Chitosan-based nanodelivery systems for cancer therapy: Recent advances.* Carbohydrate Polymers, 2021. **272**: p. 118464.
2. Yousefi, M., A. Narmani, and S.M. Jafari, *Dendrimers as efficient nanocarriers for the protection and delivery of bioactive phytochemicals.* Advances in colloid and interface science, 2020. **278**: p. 102125.
3. Narmani, A., et al., *Folic acid functionalized nanoparticles as pharmaceutical carriers in drug delivery systems.* Drug development research, 2019. **80**(4): p. 404-424.
4. Abadi, S.M.K., et al., *Anti CD19-PAMAM G4-PEG nano-complex as a potential targeted delivery system against leukemia.* Micro and Nano Systems Letters, 2025. **13**(1): p. 13.

5. Narmani, A., et al., *Smart chitosan-PLGA nanocarriers functionalized with surface folic acid ligands against lung cancer cells.* International Journal of Biological Macromolecules, 2023. **245**: p. 125554.
6. Corn, B.W. and D.B. Feldman, *Cancer statistics, 2025: A hinge moment for optimism to morph into hope?* CA: A Cancer Journal for Clinicians, 2025. **75**(1).
7. Siegel, R.L., et al., *Cancer statistics, 2025.* Ca, 2025. **75**(1): p. 10.
8. Zhao, C., et al., *Dietary risk factors and cancer mortality burden from 1990 to 2021: a comparative study of China and global regions with varying sociodemographic development levels based on the Global Burden of Disease database.* Frontiers in Nutrition, 2025. **12**: p. 1628792.
9. Rahib, L., et al., *Estimated projection of US cancer incidence and death to 2040.* JAMA network open, 2021. **4**(4): p. e214708-e214708.
10. Wu, V., et al., *Rare primary hepatic malignancies: a case-based review.* Clinical Imaging, 2021. **69**: p. 196-204.
11. Wui, W.T., *Critical Clinical Gaps in Cancer Precision Nanomedicine Development.* Current Trends in Biotechnology & Pharmacy, 2023. **17**.
12. Hsu, C.-Y., et al., *Recent advances in polysaccharide-based drug delivery systems for cancer therapy: a comprehensive review.* Artificial Cells, Nanomedicine, and Biotechnology, 2024. **52**(1): p. 564-586.
13. Elsadek, N.E., et al., *Electrospun nanofibers revisited: An update on the emerging applications in nanomedicine.* Materials, 2022. **15**(5): p. 1934.
14. Narmani, A., et al., *Gadolinium nanoparticles as diagnostic and therapeutic agents: Their delivery systems in magnetic resonance imaging and neutron capture therapy.* Journal of drug delivery science and technology, 2018. **44**: p. 457-466.
15. Narmani, A., K. Yavari, and J. Mohammadnejad, *Imaging, biodistribution and in vitro study of smart 99mTc-PAMAM G4 dendrimer as novel nano-complex.* Colloids and Surfaces B: Biointerfaces, 2017. **159**: p. 232-240.
16. Hosseini, A., et al., *Folic Acid-Chitosan-PLGA Nano Delivery System Against Liver Cancer Cells: In Vitro Studies.* Journal of Biochemical and Molecular Toxicology, 2025. **39**(9): p. e70478.

17. Zafar, A., et al., *Advancements and limitations in traditional anti-cancer therapies: a comprehensive review of surgery, chemotherapy, radiation therapy, and hormonal therapy.* Discover oncology, 2025. **16**(1): p. 607.
18. Sharma, D. and G.J. Czarnota, *Using ultrasound and microbubble to enhance the effects of conventional cancer therapies in clinical settings.* Cancer and Metastasis Reviews, 2025. **44**(1): p. 1-10.
19. Nekoueifard, E., et al., *Design and fabrication of pH-responsive charge-switchable PEG-CDM-PAMAM nanoassemblies to improve tumor therapy.* International Journal of Pharmaceutics, 2025: p. 125852.
20. Aghanejad, A., et al., *Targeted co-delivery nanosystem based on methotrexate, curcumin, and PAMAM dendrimer for improvement of the therapeutic efficacy in cervical cancer.* Scientific Reports, 2025. **15**(1): p. 1813.
21. Narmani, A., et al., *Targeting delivery of oxaliplatin with smart PEG-modified PAMAM G4 to colorectal cell line: In vitro studies.* Process Biochemistry, 2018. **69**: p. 178-187.
22. Kouhjani, M., et al., *Nose to brain delivery of insulin loaded in PLGA and chitosan-coated PLGA nanoparticles: A promising approach for Alzheimer's disease therapy.* Journal of Drug Delivery Science and Technology, 2025. **108**: p. 106857.
23. Gaur, M., et al., *Synthesis and evaluation of BSA-loaded PLGA–chitosan composite nanoparticles for the protein-based drug delivery system.* ACS omega, 2023. **8**(21): p. 18751-18759.
24. Kesharwani, P., et al., *PEGylated PLGA nanoparticles: unlocking advanced strategies for cancer therapy.* Molecular Cancer, 2025. **24**(1): p. 205.
25. Narmani, A., J. Mohammadnejad, and K. Yavari, *Synthesis and evaluation of polyethylene glycol-and folic acid-conjugated polyamidoamine G4 dendrimer as nanocarrier.* Journal of Drug Delivery Science and Technology, 2019. **50**: p. 278-286.
26. Wang, Y., et al., *Versatile PLGA-Based Drug Delivery Systems for Tumor Immunotherapy.* Small Methods, 2025: p. 2401623.
27. Donia, T., et al., *Synergistic anticancer efficacy of polydatin and sorafenib against the MCF-7 breast cancer cell line via inhibiting of PI3K/AKT/mTOR pathway and reducing resistance to treatment.* Biochemical and Biophysical Research Communications, 2024. **739**: p. 150972.

28. Wang, Q., et al., *Synergistic action of benzyl isothiocyanate and sorafenib in a nanoparticle delivery system for enhanced triple-negative breast cancer treatment.* Cancers, 2024. **16**(9): p. 1695.
29. Ahmadi, S., et al., *An injectable chitosan based dual thermo/pH-responsive fast gelling hydrogel loaded by methotrexate/curcumin as local drug delivery system of breast cancer.* Journal of Drug Delivery Science and Technology, 2025. **104**: p. 106540.
30. Nabipour, H., et al., *Novel metal-organic framework coated with chitosan-κ-carrageenan as a platform for curcumin delivery to cancer cells.* International Journal of Biological Macromolecules, 2025. **301**: p. 140027.
31. Khan, M.S., et al., *Advances in PLGA-based polymeric nanocarriers for colorectal cancer therapy: overcoming chemoresistance through controlled delivery strategies.* Molecular Cancer, 2025. **24**(1): p. 288.
32. Khakinahad, Y., et al., *Margetuximab conjugated-PEG-PAMAM G4 nano-complex: A smart nano-device for suppression of breast cancer.* Biomedical engineering letters, 2022. **12**(3): p. 317-329.
33. Fotouhi, P., et al., *Surface modified and rituximab functionalized PAMAM G4 nanoparticle for targeted imatinib delivery to leukemia cells: In vitro studies.* Process Biochemistry, 2021. **111**: p. 221-229.
34. Narmani, A., *Targeted PLGA-PAMAM Nanocarrier for efficient Doxorubicin Delivery against Pancreatic Cancer: An In Vitro Evaluation.* 2025.
35. Pourhossein, M., et al., *The theragnostic potential of polyaniline-decorated magnetic nanoparticles: a sorafenib carrier for chemo-photothermal therapy and imaging of hepatocellular carcinoma.* Journal of Drug Delivery Science and Technology, 2025: p. 107307.
36. Narmani, A., et al., *Dual targeting of breast cancer by chitosan/poly lactic-co-glycolic acid nanodelivery systems: Surface activation with folic acid/aptamers, and co-encapsulated with Sorafenib and quercetin.* Carbohydrate Polymer Technologies and Applications, 2025. **9**: p. 100695.
37. Ching, Y.C., et al., *Curcumin/Tween 20-incorporated cellulose nanoparticles with enhanced curcumin solubility for nano-drug delivery: characterization and in vitro evaluation.* Cellulose, 2019. **26**(9): p. 5467-5481.

38. Gunathilake, T.M.S.U., et al., *Enhanced curcumin loaded nanocellulose: a possible inhalable nanotherapeutic to treat COVID-19.* Cellulose, 2022. **29**(3): p. 1821-1840.
39. Saadh, M.J., et al., *Recent advances of hyaluronic acid-based materials in drug delivery systems and regenerative medicine: A review.* Archiv der Pharmazie, 2025. **358**(3): p. e2400903.
40. Ramezani, F., et al., *Folic Acid-Decorated Chitosan-PLGA Nanobiopolymers for Targeted Drug Delivery to Acute Lymphoblastic Leukemia Cells: In Vitro Studies.* Technology in Cancer Research & Treatment, 2024. **23**: p. 15330338241308077.
41. Li, J., et al., *Advances in polysaccharide-based materials for biomedical and pharmaceutical applications: A comprehensive review.* Archiv der Pharmazie, 2025. **358**(1): p. e2400854.
42. Danaei, M., et al., *Impact of particle size and polydispersity index on the clinical applications of lipidic nanocarrier systems.* Pharmaceutics, 2018. **10**(2): p. 57.
43. Dasgupta, A., et al., *Nanoparticle delivery to tumours: from EPR and ATR mechanisms to clinical impact.* Nature reviews bioengineering, 2024. **2**(9): p. 714-716.
44. Deng, X., et al., *Regulation of oxidative stress and inflammation caused by drug accumulation in the TME based on EPR-passive strategy and active targeting.* Cancer Nanotechnology, 2025. **16**(1): p. 40.
45. Hashida, M., *Advocation and advancements of EPR effect theory in drug delivery science: A commentary*. 2022, Elsevier. p. 355-357.
46. Chen, X., et al., *An EPR-independent therapeutic strategy: Cancer cell-mediated dual-drug delivery depot for diagnostics and prevention of hepatocellular carcinoma metastasis.* Biomaterials, 2021. **268**: p. 120541.
47. Amirishoar, M., et al., *Design and fabrication of folic acid-conjugated and gold-loaded poly (lactic-co-glycolic acid) biopolymers for suppression of breast cancer cell survival combining photothermal and photodynamic therapy.* Journal of Drug Delivery Science and Technology, 2023. **83**: p. 104266.
48. Sharifi, M., et al., *An updated review on EPR-based solid tumor targeting nanocarriers for cancer treatment.* Cancers, 2022. **14**(12): p. 2868.

49. Ijaz, R., et al., *Revolutionizing hypertension management: cutting-edge microneedle patch infused with zinc oxide nanoparticles for advanced transdermal drug delivery.* BioNanoScience, 2024. **14**(2): p. 1397-1409.
50. Almajidi, Y.Q., et al., *Advances in chitosan-based hydrogels for pharmaceutical and biomedical applications: a comprehensive review.* International Journal of Biological Macromolecules, 2023. **253**: p. 127278.
51. Jiang, M., et al., *Advances in preparation, biomedical, and pharmaceutical applications of chitosan-based gold, silver, and magnetic nanoparticles: a review.* International Journal of Biological Macromolecules, 2023. **251**: p. 126390.
52. Mahar, R., et al., *Application of PLGA as a biodegradable and biocompatible polymer for pulmonary delivery of drugs.* Aaps Pharmscitech, 2023. **24**(1): p. 39.
53. Maadani, A.M. and E. Salahinejad, *Performance comparison of PLA-and PLGA-coated porous bioceramic scaffolds: Mechanical, biodegradability, bioactivity, delivery and biocompatibility assessments.* Journal of Controlled Release, 2022. **351**: p. 1-7.
54. Pandya, I., et al., *Multifunctional and stimuli-responsive ionic liquid-polymeric hydrogel: a promising platform for co-drug delivery in cancer treatment.* Nanoscale, 2025.
55. Narmani, A., et al., *Biomedical applications of PLGA nanoparticles in nanomedicine: advances in drug delivery systems and cancer therapy.* Expert opinion on drug delivery, 2023. **20**(7): p. 937-954.
56. Narmani, A., et al., *Breast tumor targeting with PAMAM-PEG-5FU-99mTc as a new therapeutic nanocomplex: in in-vitro and in-vivo studies.* Biomedical Microdevices, 2020. **22**(2): p. 31.
57. Sorasitthiyanukarn, F.N., et al., *Chitosan/alginate nanoparticles as a promising approach for oral delivery of curcumin diglutaric acid for cancer treatment.* Materials Science and Engineering: C, 2018. **93**: p. 178-190.
58. Shahpouri, M., et al., *Dual-stage acting dendrimeric nanoparticle for deepened chemotherapeutic drug delivery to tumor cells.* Advanced Pharmaceutical Bulletin, 2024. **14**(3): p. 634.
59. Sadeghi, S., et al., *Biocompatible PLGA-PCL nanobeads for efficient delivery of curcumin to lung cancer.* Cancer Nanotechnology, 2024. **15**(1): p. 34.